Applied Catalysis B: Environmental 84 (2008) 440–447

Contents lists available at ScienceDirect

Applied Catalysis B: Environmental

journal homepage: www.elsevier.com/locate/apcatb

TiO_2 photoactivity in vis and UV light: The influence of calcination temperature and surface properties

Paulina Górska [a], Adriana Zaleska [a,*], Ewa Kowalska [a], Tomasz Klimczuk [b,1], Janusz W. Sobczak [c], Ewa Skwarek [d], Władysław Janusz [d], Jan Hupka [a]

[a] Department of Chemical Technology, Chemical Faculty, Gdansk University of Technology, 80-952 Gdansk, Poland
[b] Department of Solid State Physics, Faculty of Applied Physics and Mathematics, Gdansk University of Technology, 80-952 Gdansk, Poland
[c] Laboratory of Electron Spectroscopies, Institute of Physical Chemistry, Polish Academy of Sciences, 01-224 Warsaw, Poland
[d] Department of Radiochemistry and Colloid Chemistry, Faculty of Chemistry, Maria Curie-Sklodowska University, 20031 Lublin, Poland

ARTICLE INFO

Article history:
Received 1 February 2008
Received in revised form 12 April 2008
Accepted 29 April 2008
Available online 7 May 2008

Keywords:
Titanium dioxide
Heterogeneous photocatalysis
Calcination
Visible and ultraviolet light

ABSTRACT

A series of TiO_2 photocatalysts were obtained using several calcination temperatures ranging from 350 to 750 °C. The photocatalysts' characteristics by X-ray diffraction, UV–vis and FTIR diffuse reflectance spectroscopies, X-ray photoelectron spectroscopy, BET and BJH methods showed that sample active in vis region had anatase structure, about 200 m^2/g specific surface area, absorbed light for $\lambda > 400$ nm and contained 10.1 at.% of C–C species. The photocatalytic activity of the catalysts was estimated by measuring the decomposition rate of phenol in 0.21 mM aqueous solution in visible and ultraviolet light. The experimental data clearly indicate correlation between the absorption intensity of irradiation by obtained powders and their photocatalytic performance in phenol degradation. An increase in absorbance over the entire vis region and the highest photocatalytic activity for phenol degradation in visible light ($\lambda > 400$ nm) occurred for photocatalyst calcinated at 350 °C. Photocatalyst processed at 450 °C had the best activity in UV light ($250 < \lambda < 400$ nm).

1. Introduction

Significant progress, which has been made in recent years in preparation of titania-based photocatalysts to be active in visible light range, still requires better understanding of the process phenomenology. To study the subject, the sol–gel method of titanium preparation involving calcination was selected most frequently since it allows controlling to some degree the crystal size, the specific surface area and the phase composition.

TiO_2 is usually obtained by hydrolysis of titanium alkoxide, followed by annealing in the presence of oxygen. The crystalline structure decides about the band gap of semiconductor that determines light-absorption properties of TiO_2 [1]. Porter et al. [2] studied microstructural changes in commercial Degussa P-25 TiO_2 due to heat-treatment. The powder was annealed from 600 to 1000 °C. With the increasing calcination temperature the apparent crystallite size and rutile content in the catalyst increased, whereas the specific surface area and the rate of phenol photodecomposition under UV irradiation decreased. The same effect was observed by Reddy et al. [3] for photocatalysts obtained by $TiCl_4$ hydrolysis and calcination at low temperatures, between 100 and 600 °C. Inagaki et al. [4] characterized four different TiO_2 samples (ST-01, A11 and two powders obtained by TIP hydrolysis) annealed in the range from 400 to 900 °C for different periods of time. A marked increase in the crystallite size and a decrease in lattice strain were observed for catalysts annealed above 600 °C. The rate of methylene blue degradation in UV increased with increasing calcination temperature from 400 to 700 °C. Calcination above 700 °C resulted in a smaller rate constant, mainly due to partial transformation of anatase to rutile.

Various approaches to develop visible-light-activated TiO_2 have been investigated. High reactivity of the photocatalyst in visible light should allow the main part of the solar spectrum to be used. Most attempts of TiO_2 modification have concentrated in doping a catalyst with selected heteroions. It has been found that doping with non-metal atoms, such as carbon [5–7], nitrogen [8–10], sulfur [11,12], fluorine [13,14], iodine [15] and boron [16] could successfully shift or extend TiO_2 absorption properties towards visible light.

Doping with carbon atoms has attracted much attention in the last decade. It was reported that carbon could improve the activity of TiO_2, stabilize anatase structure and increase adsorption of organic molecules on the catalysts surface [5–7,17–19]. Tseng et al.

* Corresponding author. Tel.: +48 58 3472437; fax: +48 58 3472065.
E-mail address: azal@chem.pg.gda.pl (A. Zaleska).
[1] On leave at: Los Alamos National Laboratory, Los Alamos, NM 87545, USA.

0926-3373/$ – see front matter © 2008 Elsevier B.V. All rights reserved.
doi:10.1016/j.apcatb.2008.04.028

[7] studied oxidation of NO_x using own carbon-doped catalysts, which were illuminated with UV and vis light. The catalysts were prepared by the sol–gel process using titanium alkoxide and ethanol with nitric acid as a catalyst, followed by calcination at 150–600 °C. Experimental results showed that about 70% of NO_x could be removed in the presence of a modified catalyst in a continuous flow type reaction system. They stated, that the presence of carbonaceous species and mixed crystalline phase in TiO_2 powder enhances absorption of visible light by the catalyst. A significant influence of the alkyl groups was observed by Lettmann et al. [5]. TiO_2 catalysts were prepared by modified sol–gel process using different alkoxide precursors, in the absence of any dopant. Powders containing carbonaceous species revealed photocatalytic activity for 4-chlorophenol decomposition in visible light. Sakthivel and Kisch [6] also observed 4-chlorophenol degradation in the presence of a catalyst containing carbon and diffused indoor daylight. In this case, powders were prepared by hydrolysis of titanium tetrachloride with tetrabutylammonium hydroxide as a carbon precursor.

Recently, several own visible-light-activated catalysts were prepared by hydrolysis of titanium (IV) isopropoxide in the presence of thioacetamide and thiourea, followed by calcination at 450 °C [20–22]. Although aimed at investigation of the impact of non-metallic dopants, these catalysts contained carbon from two sources: TiO_2 organic precursor and dopant organic precursors. Our attempt here was to approach more holistically the impact of the preparation temperature on TiO_2 photocatalytic properties in both UV and vis regions, since further insight into the role of surface carbon in the photocatalytic activity is needed. In our research no HNO_3 was used in the preparation procedure – as described by Tseng et al. [7] – to avoid surface rutile. TiO_2 powders were calcinated at 350–750 °C. No intentionally added dopant was used. Residual carbon in photocatalysts resulted from TiO_2 precursor. Samples were characterized by XRD, XPS, DR/UV–vis and FTIR spectroscopies, potentiometric titration and by gas adsorption at 77 K. The surface properties were related to the photocatalytic activity of phenol degradation in vis and UV light.

2. Experimental

2.1. Materials and instruments

TiO_2-based catalysts were obtained, according to procedures described previously [20–22]. Titanium (IV) isopropoxide (97%, Sigma–Aldrich Co., Germany) was hydrolyzed with distilled water. The suspension was kept at 80 °C for 12 h. The precipitate was filtered, rinsed with ethanol, dried at 80 °C for 12 h and calcinated at 350, 450, 550, 650 and 750 °C for 2 h in air, referred to in the paper as *T*_350, *T*_450, *T*_550, *T*_650 and *T*_750, respectively. After calcinations, *T*_450, *T*_550, *T*_650 and *T*_750 remained white, whereas *T*_350 was brown.

The crystal structure of powders was determined from XRD patterns measured using an X-ray diffractometer (Xpert PRO-MPD, Philips) with a Cu target Kα-ray (λ = 1.5404 Å). Average crystallite size (L) and lattice strain (ε) were separately determined from the dependence of full widths at half maximum intensity (FWHMs) of the diffraction lines observed in the range of 2θ = 20–80° according to the Scherrer's equation [23].

The UV–vis/DR spectra were characterized using a UV–vis spectrometer (Jasco, V-530) equipped with the integrating sphere accessory for diffuse reflectance. $BaSO_4$ was used as reference.

ASAP 2405 instrument (Micromeritics) was used for measurements of BET surface area and pore size of the catalysts by physical adsorption and desorption of nitrogen. The S_{BET} values were calculated according to the BET method using adsorption data at relative pressures p/p_o between 0.05 and 0.25, where p and p_o denotes the equilibrium and saturation pressure of nitrogen respectively. Mesopore-size distribution was calculated with the Barrett–Joyner–Halenda method of isotherm.

Diffuse reflectance FTIR spectra were recorded using FTIR spectrometer (FT-IR 430, Jasco) equipped with Harrick diffuse-reflection attachment.

ESCALAB-210 spectrometer (VG Scientific) was used for X-ray photoelectron spectroscopy measurements—the Al Kα X-ray source operated at 300 W (15 kV, 20 mA). Survey spectra were recorded for all the catalysts in the energy range from 0 to 1350 eV with 0.4 eV step. High-resolution spectra were recorded with 0.1 eV step, 100 ms dwell time and 20 eV pass energy. 90° take-off angle was used in all measurements. AVANTAGE data system software served for curve fitting.

The point of zero charge (pzc) and surface charge density (σ) of the catalysts were determined by potentiometric titration of suspension and background electrolyte. The experiments were carried out in temperature-controlled teflon vessel (25 °C) under nitrogen atmosphere, and in 0.1; 0.01 and 0.001 M NaCl background solution. The pH values were measured using a set of glass REF 451 and calomel pHG201-8 electrodes.

2.2. Photocatalytic activity test

The photocatalytic activity was estimated by measuring the decomposition rate of 0.21 mM phenol aqueous solution in vis and UV light. Photocatalytic degradation runs were preceded with blind tests in the absence of a catalyst or illumination. Phenol was selected as a model contaminant. Phenol is present in wastewater from oil refining, pharmaceutical synthesis, electroplating, papermaking, coking and iron-smelting. Recently, phenol was proposed as one of four substrates in a multi photoactivity test [24].

25 ml of suspension containing 125 mg of a catalyst was stirred using a magnetic stirrer and aerated (5 l/h) prior and during the photocatalytic process. Four 1.0 ml aliquots of the aqueous suspension were collected during irradiation and filtered through syringe filters (∅ = 0.2 μm) to remove particles of the catalyst. The phenol concentration was estimated by the colorimetric method (λ = 480 nm) after derivatisation with diazo-*p*-nitroaniline using UV–vis spectrophotometer (DU-7, Beckman).

A schematic diagram of the experimental set-up for the photocatalyst activity testing is presented in Fig. 1. 1000 W Xenon lamp (6271H, Oriel) was used as the irradiation source. The optical path included water filter and glass filters (GG or UG) to cut off IR and vis or UV irradiation, respectively. GG400, GG420, GG455 and GG495 glass filter transmitted light of wavelength greater than 400, 420, 455 and 495 nm, whereas UG11 in the range of 250–400 nm (maximum 330 nm).

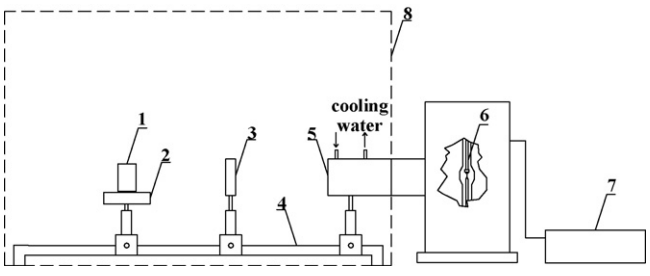

Fig. 1. Schematic diagram of the experimental set-up for examining the photocatalytic activity: 1 – cylindrical reactor with quartz window, 2 – magnetic stirrer, 3 – glass filter, 4 – optical bench, 5 – water filter, 6 – xenon lamp, 7 – power supply, 8 – black box.

3. Results

3.1. Photocatalytic activity

No degradation of phenol was observed in the absence of a catalyst or illumination. Phenol degradation efficiency results under visible light ($\lambda > 400$ nm) for powders calcinated at different temperatures are presented in Fig. 2A. Catalysts calcinated at 450, 550, 650 and 750 °C show low phenol decomposition, whereas *T*_350 sample revealed significant photocatalytic activity in visible light. After 60 min of irradiation about 80% of phenol was degraded in the presence of *T*_350. The efficiency decreased to 20% and 10% for catalysts calcinated at 450 and 550, 650 or 750 °C, respectively. Lettmann et al. [5] reported 30% of 4-chlorophenol (C_o = 0.25 mM) degradation after 100 °min irradiation ($\lambda > 400$) in the presence of a catalyst obtained by TIP hydrolysis, followed by calcination at 250 °C for 3 h. At the same time of irradiation (λ = 455 nm), Sakthivel and Kisch [6] observed 70% of TOC reduction (4-chlorophenol, C_o = 0.25 mM) for carbon-doped TiO_2 prepared by $TiCl_4$ hydrolysis with tetrabutylammonium hydroxide (calcination at 400 °C, 1 h). The authors reported that increasing calcination temperature leads to loss of photoactivity in the presence of visible light, which is in good agreement with our results.

Fig. 2B shows activity of TiO_2 powders in the presence of UV light. Sample *T*_450 was found most active in ultraviolet irradiation. After 60 min of irradiation about 80% of phenol was degraded. The efficiency decreased to about 50% for catalysts calcinated at 350, 550 and 650 °C. The lowest activity (40%) was observed for *T*_750 catalyst. The photocatalytic activity of TiO_2 under UV light and its dependence on the calcination temperature

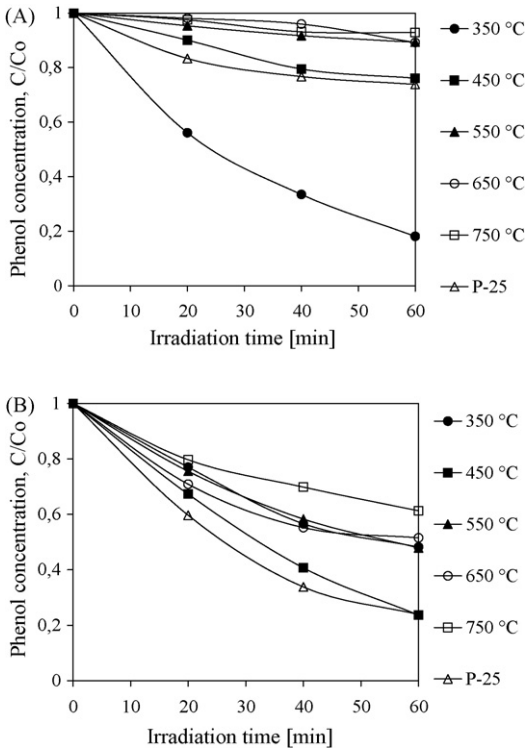

Fig. 2. Kinetics of photocatalytic degradation of phenol in the presence of the catalysts calcinated at different temperatures and Degussa P25 as a reference sample: (A) under visible light ($\lambda > 400$ nm) and (B) in the presence ultraviolet radiation ($400 > \lambda > 250$ nm). Experimental conditions: C_o = 0.21 mM, *m* (TiO_2) = 125 mg, *T* = 10 °C, Q_{air} = 5 l/h.

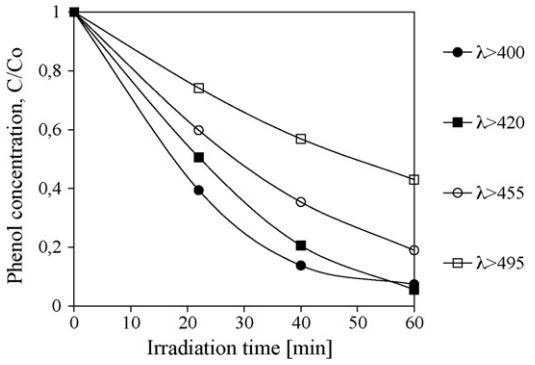

Fig. 3. Kinetics of photocatalytic degradation of phenol in the presence of *T*_350 catalyst and various wavelengths of irradiation. Experimental conditions: C_o = 0.21 mM, *m* (TiO_2) = 125 mg, *T* = 10 °C, Q_{air} = 5 l/h.

was also studied by Su et al. [1]. They reported that photodecomposition of salicylic acid (0.4 mM) reached maximum efficiency for a catalyst calcinated at 500 °C. After 100 min of irradiation about 55% of the contaminant was degraded. Samples calcinated at 400, 600 and 700 °C had lower degradation efficiency [1].

The most visible-light active catalyst (*T*_350) was evaluated in phenol degradation for selected light thresholds namely $\lambda > 400$, 420, 455 or 495 nm, see Fig. 3. The phenol degradation rates decreased with increasing irradiation wavelengths, nevertheless even for $\lambda > 495$ nm the powder was still photocatalytic active, after 60 min of irradiation over 50% of phenol was degraded. One should note differences in the efficiency of phenol degradation for sample *T*_350 presented in Figs. 2A and 3. The process efficiency presented in Fig. 2A is an average value calculated from two activity tests made for each of six independently prepared photocatalysts, while the results plotted in Fig. 3 were obtained for one selected photocatalyst.

3.2. Characteristics

3.2.1. XRD pattern

Fig. 4 illustrates the XRD patterns of samples annealed in the range from 350 to 750 °C and before calcination. Drying at 80 °C and calcination at 350, 450 and 550 °C of titania powder led to well-defined, broad, diffraction peaks corresponding to the anatase phase. Low intensity peak located at around 31° that appeared for samples *T*_350, *T*_450, *T*_550 and *T*_650 can be assigned to brookite. At 650 °C, weak reflections attributed to rutile appeared, whereas at 750 °C the crystal structure was predominantly rutile with a small amount of anatase. The literature regarding phase transformation and influence of TiO_2 crystallinity on its ultraviolet activity indicates optimal calcination temperature resulting in crystalline and highly photocatalytic active anatase phase [3]. However, titanium precursor and the synthesis conditions influence the final effect. Our most UV-active sample *T*_450 had a well-defined anatase phase. Annealing at higher temperatures (650 and 750 °C) led to deactivation of the powders due to the anatase–rutile transformation. Referring to the paper of Su et al. [1], their results indicated that low activity of samples calcinated at 600 and 700 °C was caused by phase transformation from anatase to rutile. On the other hand, the sample annealed at 400 °C was found to be anatase with amorphous titanium that is known to have low photocatalytic efficiency.

As the calcination temperature is raised, XRD reflections corresponding to the anatase phase become narrower which indicates changes of crystallite size. The average crystallite size (*L*)

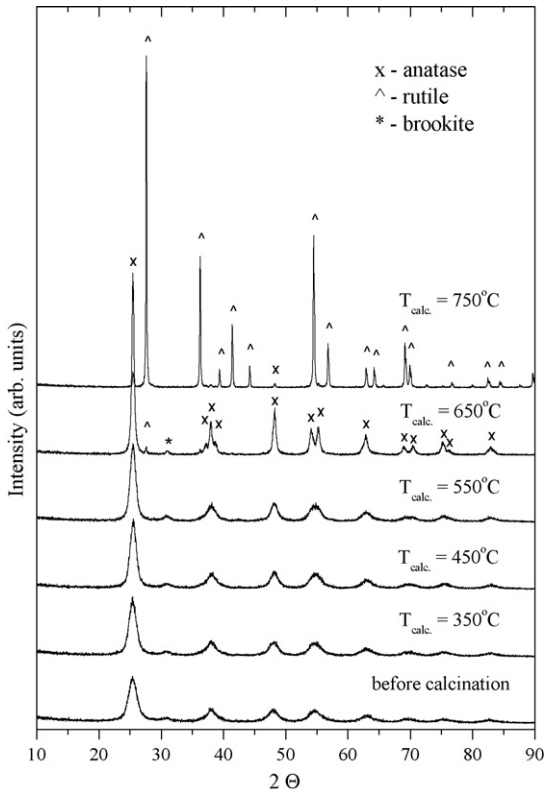

Fig. 4. X-ray diffraction pattern of the catalysts calcinated at different temperatures.

and lattice strain (ε) are presented in Fig. 5, see also Table 1. The average crystallite size of our samples treated at lower temperature (below 550 °C) increased linearly from about 8 to 11 nm (see insert in Fig. 5). Higher temperature caused rapid increase of L up to about 28 and 59 nm for samples T_650 and T_750, respectively. The lattice strain value decreased from 0.020 to 0.004 with the elevated annealing temperature. It can be seen, that samples calcinated at 350, 450 and 550 °C had almost the same L values, but ε values were different. The same effect was observed by Inagaki et al. [4] for four different samples of TiO_2 calcinated at 400 to 700 °C—changing of L value was negligible while ε value decreased rapidly. Tseng at al. [7] reported crystallite size of TiO_2 calcinated at 150–600 °C for 5 h using Scherrer's equation as we did. The crystallite size was 9.2 nm in the case of TiO_2 calcinated at 400 °C and over 50 nm in the case of TiO_2 calcinated at 600 °C. The crystal size of TiO_2 powders annealed for 2 h by Su et al. [1] increased from 4 nm for 400 °C to 35 nm for 700 °C. Our results are in good agreement with their measurements.

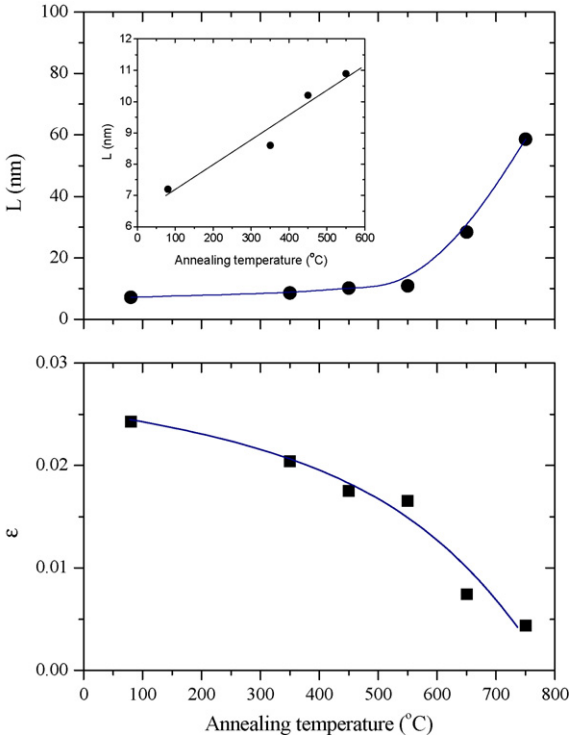

Fig. 5. Dependence of crystallite size L (upper panel) and lattice strain ε (lower panel) on the calcination temperature of the catalysts.

3.2.2. UV–vis/DR spectra

UV–vis/DR spectra for synthesized TiO_2 powders are presented in Fig. 6. The samples before calcination, T_450, T_550 and T_650 show clear absorption edge at around 350 nm and no absorption in visible region above 380 nm. The sample annealed at the lowest temperature (350 °C), exhibiting the highest photocatalytic activity in visible light, noticeably absorbs light above 380 nm. However, this sample does not show a sharp absorption edge as observed for other TiO_2 powders. In the case of T_750, a red shift of the absorption edge was observed, mainly due to the presence of rutile.

Band gap energies (E_{bg}) calculated from the first derivative of UV–vis absorption spectrum are presented in the Table 1. The band gap energy value changed from 3.41 to 3.04 eV thus it was narrowing with increasing calcination temperature. Usually E_{bg} values reported in the literature for anatase are around 3.2 eV [25]. Band gap energy of our anatase samples was in the range of 3.3 eV. According to Saupe et al. [26], a combination of quantum size effects due to crystallite size and the dopant atoms in the structure, give a wider band gap than TiO_2 bulk. On the other hand, lower value of band gap energy for samples T_650 and T_750 is a result of anatase/rutile phase transformation; see XRD spectra in Fig. 4. The literature reports 3.0 eV for pure rutile phase [25].

3.2.3. BET surface area

TiO_2 photoactivity depends on surface properties of the catalyst. Samples calcinated at 350 and 450 °C have the highest BET surface area of about 200 and 180 m^2/g and the lowest average pore diameters of about 8 and 9 nm, respectively. As the calcination temperature increases, BET surface area of TiO_2 decreases progressively, reaching the lowest value equal to 8.3 m^2/g at T = 750 °C, whereas average pore diameter increases (Table 1). The biggest pore diameter (14 nm) is obtained for T_750.

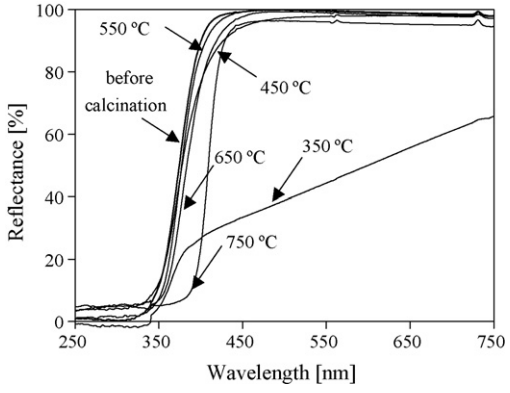

Fig. 6. UV–vis/DR spectra for the catalysts calcinated at different temperatures.

Table 1
Characteristics of the catalysts calcinated at different temperatures

	*T*_350	*T*_450	*T*_550	*T*_650	*T*_750
Annealing temperature (°C)	350	450	550	650	750
Average crystallite size, *L* (nm)	8.4	10.2	10.9	28.4	58.6
Lattice strain, ε	0.020	0.018	0.017	0.007	0.004
Band gap energy (eV)	3.41	3.33	3.31	3.27	3.04
BET surface area (m^2/g)	205.8	180.2	147.7	93.5	8.3
Langmuir surface area (m^2/g)	262.6	229.7	201.3	129.3	11.8
BJH cumulative adsorption surface area of pores between 1.7 and 300 nm diameter (m^2/g)	259.3	225.5	183.2	115.1	9.5
BJH cumulative desorption surface area of pores between 1.7 and 300 nm diameter (m^2/g)	285.0	252.8	218.2	127.5	11.2
Average pore diameter (4V/A by BET) (nm)	8.3	9.4	11.0	11.0	14.0
BJH adsorption on average pore diameter (4V/A) (nm)	6.8	7.9	9.2	9.1	14.7
BJH desorption on average pore diameter (4V/A) (nm)	6.1	6.9	7.6	8.1	11.5
Pore volume (cm^3/g)	0.43	0.43	0.40	0.26	0.03
Point zero charge	4.5	4.5	4.5	4.5	6.0

Surface area decrease resulted from sintering and crystal growth of catalyst particles [17]. Relations between photoactivity in vis and UV region versus BET surface area are shown in Fig. 7. Photoactivity is presented as phenol degradation efficiency after 60 min of irradiation in vis or UV light. The efficiency of phenol degradation in the presence of visible light ($\lambda > 400$ nm) increases with increasing surface area of catalysts. In the case of UV light, it reaches maximum for the *T*_450 sample with specific surface area equal to about 180 m^2/g. It indicates that in the case of UV-activity other parameters cause its enhancement.

3.2.4. FTIR/DR spectra

Fig. 8 displays FTIR/DR spectra for the photocatalysts. Peak observed at 1633 cm^{-1} is assigned to water molecules. The broad and strong absorption bands covering 2500–3700 cm^{-1} region are ascribed to hydroxyl groups chemisorbed on the TiO_2 surface and dissociated or molecularly adsorbed water [10,18]. Generally, the increase in calcination temperature leads to reducing the intensities of the bands. Such results were observed by Kuroda et al. [10] who heated $TiO_{2-x}N_x$ at various temperatures in the range of 100–350 °C and Janus et al. [18] for the C-doped samples heated from 150 to 400 °C. The sample before calcination reveals bands in 2800–3100 cm^{-1} region and at about 1380 cm^{-1}, assigned to $-CH_3$ groups. Janus et al. [18] also observed $-CH_3$ groups for their catalyst modified with ethanol and calcinated even at 400 °C. In our case the bands disappeared after calcination.

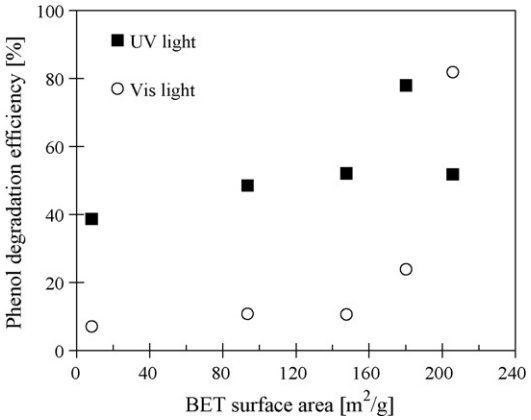

Fig. 7. Dependence of BET surface area of photocatalysts on the photoactivity under vis and UV light. Photoactivity estimated as phenol degradation efficiency after 60 min irradiation.

3.2.5. XPS analysis

The atomic composition of investigated TiO_2 powders was analyzed by XPS. Table 2 shows atomic ratio of TiO_2 samples calcinated at 350–750 °C. The Ti 2p spectrum could be resolved into two components at binding energies ~459 and ~458 eV and are identified with TiO_2 and Ti_2O_3, respectively. Intensities of the decomposed components suggest that Ti^{4+} is the dominant surface state. Sample *T*_350 mainly contains Ti^{4+} and the least amount of reduced species in the form of Ti^{3+} ions. For TiO_2 annealed at temperatures from 450 to 750 °C, the Ti^{4+}:Ti^{3+} ratio was from 38:1 to 26:1, respectively (see Table 2). The lowest Ti^{4+}:Ti^{3+} (23:1) ratio was observed for TiO_2 sample calcinated at medium temperature – 550 °C. Regarding the literature data, O 1s peak could be composed of 3–5 different species, such as Ti–O bonds in TiO_2 and Ti_2O_3, hydroxyl groups, C–O bond, and adsorbed H_2O [27]. In our investigation three peaks were identified. The first peak at about 533 eV was related to oxygen in carboxyl group, the second peak at about 532 eV was related to surface hydroxyl groups and the third peak at about 530 eV indicated oxygen in the TiO_2 crystal lattice. Comparison of XPS spectra for O 1s region for samples calcinated from 350 to 750 °C is provided in Fig. 9A. The ratio between lattice oxygen to surface oxygen species is given in Table 2. The lowest value was observed for *T*_450. Calcination at 550, 650 and 750 °C resulted in many a number of lattice oxygen species. XPS analysis enabled detection of carbonaceous species on the TiO_2 surface, see Fig. 9B. C–C, C–OH, C═O and COOH peaks appeared at 284–289 eV, where the surface C–C structures were best represented. According to the literature, incorporation of carbonaceous species (C–C) occur in highly condensed and coke-like structure, so it could play the

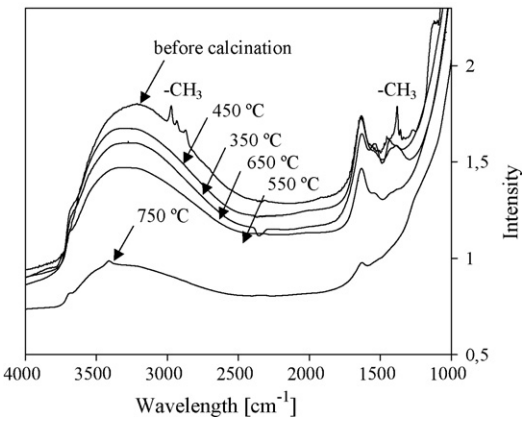

Fig. 8. FTIR/DR spectra for the catalysts calcinated at different temperatures.

Table 2
Atomic composition of the catalysts calcinated at different temperatures

Annealing temperature (°C)	Ti^{4+}:Ti^{3+} ratio	Oxygen ratio: lattice/surface	Carbon content (at.%)		Composition
			Total	C–C species[a]	
350	53:1	7.7:1	15.2	10.1	$TiO_{2.57}C_{0.66}$
450	38:1	6.6:1	9.4	5.2	$TiO_{2.80}C_{0.41}$
550	23:1	9.5:1	13.0	9.7	$TiO_{2.67}C_{0.57}$
650	39:1	10.1:1	8.5	6.1	$TiO_{2.45}C_{0.33}$
750	26:1	9.8:1	12.7	9.1	$TiO_{2.42}C_{0.52}$

[a] Binding energy equal 285.0 eV.

role of sensitizer to induce the visible-light absorption and response [5,7]. Carbon content in the surface layer varies from 8.5 to 15.2 at.%, see Table 2. We did not observe correlation between total surface carbon content and visible radiation-induced activity but catalysts containing more carbonaceous C–C species clearly showed better activity (see Table 2). In the case of UV irradiation, the best photoactivity had *T*_450 sample with moderate amount of carbon (9.4 at.%). The *T*_350 sample containing the highest amount of carbon, 15.2 at.% (mainly as C–C species), was most active in visible light. In comparison, Lettmann et al. [5] noticed significant 4-chlorophenol degradation in visible light for C-doped powders containing 0.6 wt.% of carbon. According to these results, authors suggested that carbon residues formed during calcination could be responsible for the photosensitization. Sakthivel and Kisch [6] reported 0.4 wt.% as the optimum carbon value responsible for visible-light activity. They found that carbon in the form of carbonate is not responsible for activity.

3.2.6. Surface charge density

The adsorption of an organic molecule at the surface of metal oxide/aqueous electrolyte systems is a complex phenomenon because it depends on the interaction between a molecule and surface groups [28]. Considering such interaction one should take into account surface charge (or groups that form such charge) and molecule form in bulk of the solution. Phenol behaves in an aqueous phase as weak acid, its pK_a = 9.89. In an aqueous solution for which pH < pK_a phenol is present in neutral form, but for pH > 9.89 anionic form of phenol prevails. Bekkouche at al. [29] show that maximum adsorption of phenol at TiO_2/aqueous solution occurs at pH_{iep}. Similar adsorption behaviour was observed for phenolic compounds using activated carbon [28].

The point of zero charge values presented in Table 1 are equal to 4.5 for samples *T*_350, *T*_450, *T*_550 and *T*_650. In a case of the sample annealed at 750 °C the point of zero charge was found at pH 6. The point of zero charge for anatase and rutile reported in the literature ranges from 2 to 8.9 as reviewed by Kosmulski [30]. The average pzc of anatase equals 5.9 and is slightly bigger than that of rutile (5.4). Our anatase samples calcinated at 350–550 °C revealed lower than the average pzc values. The value of pH_{pzc} depends on the alkali–acid character of surface hydroxyl groups and results from chemical variety of the surface, mainly by the presence of other than hydroxyl groups. These groups may be more alkaline or acidic than hydroxyl ones and shift the point of zero charge. For example, contamination by halogen ions gives easier dissociation of H^+ from such surface groups (≡SHX, where X means halogen and SH is the molecule of the solvent)—increase of negative charge density and shift of pzc is observed towards lower pH values [31]. Surface analysis performed by XPS technique confirmed that our samples annealed at 350–650 °C contained traces of chlorine, fluorine, sulfur and nitrogen. The presence of those impurities could shift the position of pzc towards lower pH. In the case of sample *T*_750 impurities could be partly removed regarding higher calcination temperate results in higher pzc value (pH_{pzc} 6).

The dependence of surface charge density (σ) versus pH for the photocatalyst/aqueous NaCl solution (0.1 M) is plotted in Fig. 10. A significant surface charge density, ranging from 10 to 20 μC/m^2, and the influence of background electrolyte concentration on charge quantity were observed. The surface charge density is most pronounced for the *T*_350 sample and decreases with growing temperature of calcination. The lowest charge density was observed for the *T*_750 sample. The surface charge density at the titania/aqueous electrolyte interface depends on the reactivity

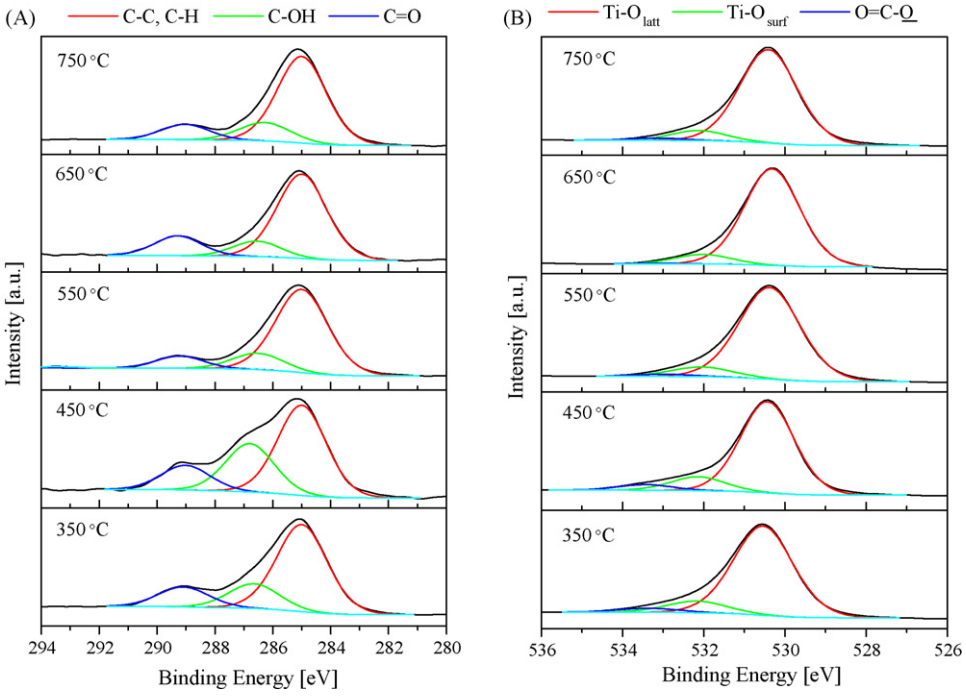

Fig. 9. XPS spectra of the catalysts calcinated at different temperatures: (A) C 1s region and (B) O 1s region.

Table 3
Visible-light activity and selected properties of *T*_350 catalyst and catalysts prepared by intentional non-metal doping (5 wt.% of thiourea or thioacetamide added during hydrolysis)

Sample no.	Kind of dopant	Calcination temperature (°C)	Surface composition (at.%)				Phase composition	Band gap energy (eV)	Phenol degradation reaction rate (μmol dm^{-3} min^{-1})
			Total carbon	C–C species	*S*	*N*			
TA5[a]	Thioacetamide	450	6.4	3.7	0.16	1.24	Anatase	3.36	2.4
TH5[a]	Thiourea	450	7.2	2.8	0.33	1.3	Anatase	3.37	2.9
*T*_350	No dopant	350	15.2	10.1	–	–	Anatase	3.41	2.8

[a] Earlier own data, see [22].

of hydroxyl groups, characterized by p*K* values, and the number of hydroxyl groups per nm^2. The comparison of relationships depicted in Fig. 10 and characteristic OH peak at 1633 cm^{-1} and bands covering 2500–3700 cm^{-1} region in Fig. 8 lead to the conclusion that calcination reduced the number of hydroxyl groups at the titania surface.

4. Discussion

Among all obtained powders, the highest visible-light activity was observed for the powder calcinated at 350 °C. Since surface area and pore size distribution are important factors for heterogeneous photocatalysis, the sample *T*_350 had the biggest BET surface area (205.8 m^2/g) and the smallest both crystallite size (8.4 nm) and average pore diameter (8.3 nm). The large surface area of *T*_350 may contribute to its enhanced activity, but cannot be responsible for 60% better phenol degradation efficiency compared to the *T*_450 sample with surface area equal to 180 m^2/g. Enhanced visible-light activity results rather from the presence of carbon, mainly in the form of C–C species, as well as from high surface area. Carbon content (15.2 at.%) in *T*_350 catalyst exceeds contents in others samples. Although, there is no red shift observed for sample *T*_350, it exhibited better light absorption in vis—moreover, the absorption tail was extended to 750 nm.

Ultraviolet activity of samples *T*_350, *T*_550 and *T*_650 was comparable and resulted in 50% degradation of phenol in 60 min and these photocatalysts differed by surface area, pore diameter and carbon content. The lattice to surface oxygen ratio changed from 6, 8 to 7 for *T*_350, *T*_550 and *T*_650, respectively, while the highest ratio of surface oxygen to lattice oxygen was observed for *T*_450 sample with the best activity in UV light (see Table 2). Since hydroxyl radicals were formed on the surface of TiO_2 by the reaction of holes with adsorbed H_2O, hydroxide, or surface titanol groups (>TiOH), high surface/lattice oxygen ratio could be responsible for the enhanced activity of sample *T*_450 in phenol degradation in UV light. The sample calcinated at 450 °C, which revealed the highest activity under UV light, had well crystallized anatase phase, high BET surface area (180 m^2/g) and average crystallite size of about 10 nm. The surface carbon concentration was estimated to be 9.4 at.%, which corresponds to the average carbon content of remaining samples.

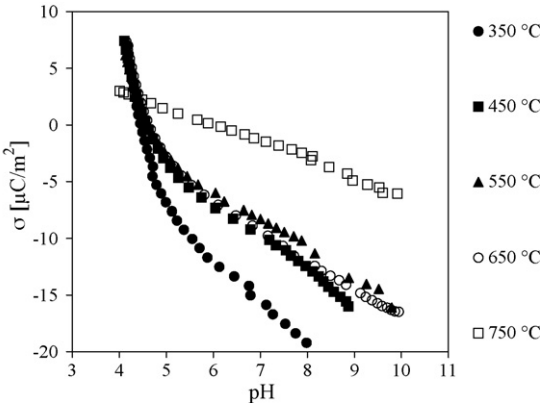

Fig. 10. Surface charge density (σ) at the photocatalyst/0.1 M NaCl solution interface as a function of pH.

Much lower visible-light activity of sample *T*_450 than *T*_350 could result not only from lower C–C species content but also from presence of oxygen vacancies. The Ti^{3+} to Ti^{4+} ratio is greater for *T*_450 than for *T*_350 (see Table 2). According to Kamisaka et al. [32] theoretical study, oxygen vacancies fill the in-gap impurity states by emitting electrons. Therefore, these oxygen vacancies are considered to suppress the formation of electron holes in the conduction band from visible light. Consequently, introduction of oxygen vacancies into carbon-doped TiO_2 is expected to suppress the photocatalytic degradation of organic molecules.

Data presented in Table 3 suggest that the *T*_350 catalyst exhibited similar visible-light activity with respect to catalysts prepared by intentional non-metal doping (thiourea or thioacetamide added during hydrolysis) and treated at a higher temperature (450 °C). TA5 and TH5 catalysts were prepared in our previous investigation by the same preparation procedure [22]. Moreover, *T*_350 catalyst allows more simple preparation procedure, and does not contain intentionally introduced elements, therefore, is more acceptable for industrial applications and the following disposal/reuse.

In this regard, presented data allow TiO_2 preparation with predictable photoactivity under UV or visible light. Lower temperature of calcination (around 350 °C) favors larger surface area, more residual carbon in the form of carbonaceous C–C species (working as sensitizers), elimination of oxygen vacancies and promotion of photoactivity under visible light. The rising temperature to 450 °C diminishes the amount of carbonaceous species and suppresses the activity under visible light. However, enhanced activity under UV light due to the compromise among surface area, crystallinity, crystal defects and content of impurities is observed. Large surface area is usually associated with numerous crystalline defects, which promote recombination of electrons and positively charged holes, leading to lower activity under UV irradiation. More elevated temperature results in diminished photoactivity due to the decrease of surface area, increase of crystallite size, formation of rutile and drop of surface oxygen content.

5. Conclusions

1. TiO_2 powder calcinated at 350 °C was most active in phenol degradation in vis light ($\lambda > 400$ nm), while the photocatalyst treated at 450 °C had the best activity in UV light ($250 < \lambda < 400$ nm, $\lambda_{max} = 330$ nm). *T*_350 contained the biggest amount of carbon in aromatic C–C bonds (10.1 at.%), known as chromophores. This explains the most effective light absorption in vis region, leading to very good degradation rate of 2.8 μmol dm^{-3} min^{-1} for phenol.

2. The experimental data confirm earlier observations, that lack of band gap narrowing with simultaneous increase of the absorption intensity still can lead to effective degradation of organic compounds, which is controlled by presence of sensitizers (residual carbon).

Acknowledgments

This work was supported by Gdansk University of Technology (contract no.: BW 014694/039) and Ministry of Science and Higher Education (contract no.: 3T09D 00826 and N205 077 31/3729). Dr. Beata Tryba (Department of Water Technology and Environmental Engineering, Szczecin University of Technology) is gratefully acknowledged for assistance in UV–vis/DR and FTIR/DR spectroscopies.

References

[1] C. Su, B.Y. Hong, C.M. Tseng, Catal. Today 96 (2004) 119–126.
[2] J.F. Porter, Y. Li, C.K. Cahn, J. Mater. Sci. 34 (1999) 1523–1531.
[3] K.M. Reddy, C.V.G. Reddy, S.V. Manorama, J. Solid State Chem. 158 (2001) 180–186.
[4] M. Inagaki, R. Nonaka, B. Tryba, A.W. Morawski, in: Proceedings of 4th International Conference Oils and Environment AUZO 2005, June 20–23, Gdansk, Poland, (2005), pp. 325–332.
[5] C. Lettmann, K. Hildenbrand, H. Kisch, W. Macyk, W.F. Maier, Appl. Catal. B 32 (2001) 215–227.
[6] S. Sakthivel, H. Kisch, Angew. Chem. Int. Ed. 42 (2003) 4908–4911.
[7] Y. Tseng, C. Kuo, C. Huang, Y. Li, P. Chou, C. Cheng, M. Wong, Nanotechnology 17 (2006) 2490–2497.
[8] H. Irie, Y. Watanabe, K. Hashimoto, J. Phys. Chem. B 107 (2003) 5483–5486.
[9] S. Sakthivel, M. Janczarek, H. Kisch, J. Phys. Chem. B 108 (2004) 19384–19387.
[10] Y. Kuroda, T. Mori, K. Yagi, N. Makihata, Y. Kawahara, M. Nagao, S. Kittaka, Langmuir 21 (2005) 8026–8034.
[11] T. Umebayashi, T. Yamaki, S. Tanaka, K. Asai, Chem. Lett. 32 (2003) 330–331.
[12] T. Ohno, M. Akiyoshi, T. Umebayashi, K. Asai, T. Mitsui, M. Matsumura, Appl. Catal. A 265 (2004) 115–121.
[13] T. Yamaki, T. Sumita, S. Yamamoto, J. Mater. Sci. Lett. 21 (2002) 33–35.
[14] A. Hattori, M. Yamamoto, H. Tada, S. Ito, Chem. Lett. 27 (1998) 707–708.
[15] X. Hong, Z. Wang, W. Cai, F. Lu, J. Zhang, Y. Yang, N. Ma, Y. Liu, Chem. Mat. 17 (2005) 1548–1552.
[16] H. Geng, S. Yin, X. Yang, Z. Shuai, B. Liu, J. Phys. :Condens. Matter 18 (2006) 87–96.
[17] T. Tsumura, N. Kojitani, I. Izumi, N. Iwashita, M. Toyoda, M. Inagaki, J. Mater. Chem. 12 (2002) 1391–1396.
[18] M. Janus, M. Inagaki, B. Tryba, M. Toyoda, A.W. Morawski, Appl. Catal. B 63 (2006) 272–276.
[19] A.W. Morawski, M. Janus, B. Tryba, M. Inagaki, K. Kałucki, C. R. Chimie 9 (2006) 800–805.
[20] P. Górska, A. Zaleska, E. Kowalska, J. Hupka, Pol. J. Chem. Tech. 8 (2006) 102–105.
[21] P. Górska, A. Czoska, A. Zaleska, J. Hupka, in: Proceedings of 4th International Conference Oils and Environment AUZO 2005, June 20–23, Gdansk, Poland, (2005), pp. 375–380.
[22] A. Zaleska, P. Górska, J.W. Sobczak, J. Hupka, Appl. Catal. B 76 (2007) 1–8.
[23] P. Scherrer, Götting. Nachr. 2 (1918) 98.
[24] W. Choi, J. Ryu, in: Proceedings of Second International Conference on Semiconductor Photochemistry, July 2–25, Aberdeen, Scotland, 2007.
[25] M.R. Hoffmann, S.T. Martin, W. Choi, D.W. Bahnemann, Chem. Rev. 95 (1995) 69–96.
[26] G.B. Saupe, T.Y. Zhao, J. Bang, N.R. Desu, G.A. Carballo, R. Ordonem, T. Bubphamala, Microchem. J. 81 (2005) 156–162.
[27] J. Yu, X. Zhao, Q. Zhao, Thin Solid Films 379 (2000) 7–14.
[28] A. Dabrowski, P. Podkoscielny, Z. Hubicki, M. Barczak, Chemosphere 58 (2005) 1049–1070.
[29] S. Bekkouche, M. Bouhelassa, N. Hadj Salah, F.Z. Meghlaoui, Desalination 166 (2004) 355–362.
[30] M. Kosmulski, Adv. Colloid Interface Sci. 99 (2002) 255–264.
[31] W. Janusz, A. Sworska, J. Szczypa, Colloid Surf. A 152 (1999) 223–233.
[32] H. Kamisaka, T. Adachi, K. Yamashita, J. Chem. Phys. 123 (2005) 084104.